**IWSSIP 2010 – 17th International Conference on Systems, Signals and Image Processing**

# Low-Redundancy Transceivers for Wireless Networks

Wallace A. Martins and Paulo S. R. Diniz
LPS – Signal Processing Laboratory
COPPE & DEL-Poli/Federal University of Rio de Janeiro
Rio de Janeiro, Brazil
Email: {wallace,diniz}@lps.ufrj.br

*Abstract*—Traditional designs of multicarrier transceivers require an amount of redundancy of at least the order of the channel. This redundancy eliminates the inherent interblock interference (IBI) and allows the exploitation of the resulting channel matrix to design superfast zero-forcing (ZF) and minimum mean-square error (MMSE) equalizers. Although it is well known that the minimum redundancy for IBI-free designs of memoryless linear and time-invariant (LTI) transceivers is around half of the channel order, all practical solutions do not employ minimum redundancy. This paper reviews in a unified way a family of block transceivers with superfast implementations employing the minimum redundancy. The related structures of practical ZF and MMSE receivers are presented and their performances are compared in terms of throughput for fixed bit-error rate (BER). The main feature of these transceivers is their higher throughput allowing the use of the wireless channels more effectively.

***Keywords*—Block transceivers; displacement; equalization; minimum redundancy; OFDM; superfast algorithms.**

## I. Introduction

The efficient use of the scarce radio-frequency band requires smart transceiver designs. The evolution of modern communications systems is driven by a search for new techniques that enable an efficient bandwidth usage. In general, this efficiency may be translated into either higher throughputs or higher system capacity. However, all these features are constrained by the available budget, calling for "simple" solutions.

The orthogonal frequency-division multiplex (OFDM) is a representative example of physical-layer technique that contributes to the aforementioned evolution. In fact, the OFDM enhances the throughput performance of previous systems, such as single-carrier transceivers based on either time- or code-division multiple accesses. In addition, the OFDM is extremely easy to implement in digital transmissions, since it uses fast Fourier transform algorithms and single-tap equalizers.

The widespread adoption of OFDM-based multicarrier transceivers confirms that efficient implementation is a necessary requirement. Wireless local and metropolitan area networks (WLAN and WMAN) following the families IEEE 802.11x and IEEE 802.16x standards, most modern digital television systems, wired Internet connections using digital subscriber lines (xDSL), and the downlink of the 3G-LTE system are all based on OFDM.

Nevertheless, OFDM-based systems have also some drawbacks. Indeed, the OFDM transceivers employ a given number of redundant elements (data that, a priori, do not contain any additional information), reducing the effective data rate or throughput. The redundancy is utilized by the transmission/reception processing to cope with the effects of the distortion introduced by frequency-selective channels. In fact, for a finite-impulse response (FIR) channel model with order $L$, the OFDM introduces at least $L$ redundant elements before the transmission. This is an issue that reduces the throughput of the transceivers, especially when the channel is very dispersive (large $L$).

The OFDM system can be cast as a particular case of FIR transmultiplexers. A general theory regarding the use of redundancy in FIR transmultiplexers was first developed in [1], [2], [3], with some further improvements described in [4]. When dealing with memoryless LTI transmultiplexers, which are the simplest FIR transmultiplexers, the authors in [2] proved that the minimum required redundancy is only $\lceil L/2 \rceil$, instead of $L$.

In this paper, we review some recent advances in the design of memoryless LTI transmultiplexers with minimum redundancy. The resulting transceivers may be multicarrier or single-carrier, with either ZF or MMSE receivers. In addition, the transceivers only employ diagonal matrices and superfast transforms, such as discrete Fourier and Hartley transforms (DFT and DHT). For this reason, the transceivers are computationally as simple as OFDM-based systems,[1] while being much more efficient with respect to the bandwidth usage.

## II. Transmultiplexers

The filter-bank transceivers, also known as transmultiplexers, are key building blocks for both single-carrier and multicarrier communications systems. They are important due to their efficiency for data transmissions through channels with moderate to severe intersymbol interference (ISI) [1], [5].

As described in [2], [5], any block-based transmultiplexer may be represented by a transmitter matrix $\mathbf{F}(z) \in \mathbb{C}^{N\times M}[z^{-1}]$, a receiver matrix $\mathbf{G}(z) \in \mathbb{C}^{M\times N}[z^{-1}]$ and a pseudo-circulant channel matrix $\mathbf{H}(z) = \mathbf{H}_{\rm ISI} + z^{-1}\mathbf{H}_{\rm IBI} \in \mathbb{C}^{N\times N}[z^{-1}]$. The dimensions of such matrices are determined by both the number of data symbols $M \in \mathbb{N}$ in a block, and

[1] Considering the asymptotic amount of complex-valued multiplications and additions used in their implementations.

the total length $N \in \mathbb{N}$ of the transmitted block, including $K = N - M$ redundant elements. The matrices $\mathbf{F}(z)$ and $\mathbf{G}(z)$ are the polyphase matrices of the transmultiplexer. Furthermore, given an $L$th-order channel model, the matrix $\mathbf{H}_{\mathrm{ISI}}$ models the ISI effect within a transmitted block, whereas the matrix $\mathbf{H}_{\mathrm{IBI}}$ models the IBI effect between two consecutive blocks, where it was assumed that $L < N$ [4]. The reader should refer to [1], [2] for detailed definitions of such matrices.

The memoryless LTI transmultiplexer is modeled by $\mathbf{F}(z) = \mathbf{F}$ and $\mathbf{G}(z) = \mathbf{G}$ for all blocks, considering the channel time-invariant. Traditional OFDM-based systems are special cases of block-based memoryless LTI transmultiplexers. Lin and Phoong [2] showed that the redundancy $K$ of an IBI-free memoryless LTI transmultiplexer must satisfy the inequality $2K \geq L$. They proposed a general parametrization for such systems, as well as a very useful special case of reduced-redundancy systems. This special case, also known as zero-padding zero-jamming (ZP-ZJ) transceiver, is characterized by the following transmitter and receiver matrices, respectively [2]: $\mathbf{F} = [\,\mathbf{F}_0^T \quad \mathbf{0}_{M\times K}]^T$, where $\mathbf{F}_0 \in \mathbb{C}^{M\times M}$, and $\mathbf{G} = [\,\mathbf{0}_{M\times(L-K)} \quad \mathbf{G}_0\,]$, where $\mathbf{G}_0 \in \mathbb{C}^{M\times(M+2K-L)}$.

When the ZP-ZJ system with reduced redundancy is employed, the resulting transceiver can be simplified as a transmitter matrix $\mathbf{F}_0$, a receiver matrix $\mathbf{G}_0$ and an effective channel matrix $\mathbf{H}_0 \in \mathbb{C}^{(M+2K-L)\times M}$. This effective channel matrix is a Toeplitz matrix with first row given by $[\,h(K) \;\; h(K-1) \;\; \cdots \;\; h(0) \;\; \mathbf{0}_{1\times(M-K-1)}\,]$ and first column given by $[\,h(K) \;\; h(K+1) \;\; \cdots \;\; h(L) \;\; \mathbf{0}_{1\times(M+3K-2L-1)}\,]^T$ [2]. In this work, we shall focus on the minimum-redundancy case, i.e., $K = L/2$, where $L$ is assumed to be even [7]. Note that, with this choice, $\mathbf{F}_0$, $\mathbf{H}_0$, and $\mathbf{G}_0$ are all square matrices.

The ZF and the MMSE linear receivers are commonly used to generate an estimate $\hat{\mathbf{s}}$ of the transmitted vector $\mathbf{s}$. Such solutions are respectively characterized by the following pair of receiver matrices:

$$\mathbf{G}_0^{\mathrm{ZF}} = (\mathbf{H}_0\mathbf{F}_0)^{-1} = \mathbf{F}_0^{-1}\mathbf{H}_0^{-1} \quad (1)$$

$$\mathbf{G}_0^{\mathrm{MMSE}} = (\mathbf{H}_0\mathbf{F}_0)^H \left[(\mathbf{H}_0\mathbf{F}_0)(\mathbf{H}_0\mathbf{F}_0)^H + \frac{\sigma_v^2}{\sigma_s^2}\mathbf{I}\right]^{-1} \quad (2)$$

where, for the ZF solution, it is assumed that $\mathbf{H}_0\mathbf{F}_0$ is invertible, whereas for the MMSE solution it is considered that the symbols and the additive noise at the receiver front-end stem from independent white random process with zero mean and variances $\sigma_s^2, \sigma_v^2 \in \mathbb{R}_+$, respectively.

We are able now to define two fundamental tasks: equalization and receiver design. In this work, equalization is defined as the multiplication of a received vector by the receiver matrix. Hence, this task requires $\mathcal{O}(M^2)$ numerical operations for unstructured matrices. On the other hand, the receiver design consists in computing the matrices $\mathbf{G}_0^{\mathrm{ZF}}$ or $\mathbf{G}_0^{\mathrm{MMSE}}$. Such a task requires $\mathcal{O}(M^3)$ numerical operations for generic matrices, considering that channel-state information (CSI) is available at the receiver end, and assuming that the transmitter matrix $\mathbf{F}_0$ had been previously defined.

Traditional OFDM-based systems perform both tasks with $\mathcal{O}(M\log_2 M)$ numerical operations, when $M$ is a power of two. These superfast solutions are achieved because OFDM-based transceivers benefit from the circulant shape that is induced in the effective channel matrix, allowing the spectral decomposition of such a matrix through DFT (eigenvector matrix) and the channel-frequency response (eigenvalues) [1]. Nevertheless, it is also possible to implement low-redundancy transceivers using a reduced amount of numerical operations. This paper reviews some approaches related to how to exploit the Toeplitz structure present in the effective channel matrix $\mathbf{H}_0$ in order to produce solutions for the equalization task related to memoryless LTI transmultiplexers, using only $\mathcal{O}(M\log_2 M)$ operations. It is possible to perform the receiver-design task using only $\mathcal{O}(M\log_2^2 M)$ operations, as described in [10].

## III. Structured-Matrix Representations

Several engineering problems induce structural patterns in their matrix representations. These structural patterns provide efficient means for exploiting features of the problem that they model. Moreover, operations involving structured matrices can be simplified by taking into account the structural patterns. Consider, for example, the sum of two $M \times M$ circulant matrices. If one ignores the structural patterns present in such matrices, then this operation will require $M^2$ additions. However, if one does consider the structure of the matrices, then this operation will require only $2M$ addition corresponding to the sum of the first rows of each matrix. Thus the resulting circulant matrix can be built by rearranging the elements of the resulting vector accordingly.

A useful tool for exploiting the structure of a matrix is the displacement approach [6]. The displacement-rank theory reveals how many parameters a given structured matrix depends on. To do so, the first step of the displacement approach is to generate a reduced-rank matrix through a linear mapping of the original structured matrix. This reduced rank is the so-called *displacement rank*. After this *compression* stage, computations with the resulting matrix with smaller rank can be performed efficiently, since there is a reduced amount of parameters to *operate on*. After all, the required result can be assessed by inverting, when possible, the displacement linear operation. The latter process is called *decompression*.

Formally, by considering that $\mathbf{X}, \mathbf{Y}, \mathbf{U} \in \mathbb{C}^{M\times M}$, the linear transforms $\nabla_{\mathbf{X},\mathbf{Y}}(\mathbf{U}) = \mathbf{X}\mathbf{U} - \mathbf{U}\mathbf{Y}$ and $\Delta_{\mathbf{X},\mathbf{Y}}(\mathbf{U}) = \mathbf{U} - \mathbf{X}\mathbf{U}\mathbf{Y}$ are the so-called *Sylvester and Stein displacement operators*, respectively [6]. When applied to a structured matrix $\mathbf{U}$, these linear maps, e.g. $\nabla_{\mathbf{X},\mathbf{Y}}$, may generate a new matrix with smaller rank. Usually, such a new matrix is represented by $\nabla_{\mathbf{X},\mathbf{Y}}(\mathbf{U}) = \mathbf{P}\mathbf{Q}^T$, with $(\mathbf{P},\mathbf{Q}) \in \mathbb{C}^{M\times S} \times \mathbb{C}^{M\times S}$ and $\mathrm{rank}\{\nabla_{\mathbf{X},\mathbf{Y}}(\mathbf{U})\} = R \leq S \ll M$.

A good illustration of the displacement approach is the compression of a square Toeplitz matrix. Consider an operator matrix $\mathbf{Z}_\lambda = [\,\mathbf{e}_2 \;\; \cdots \;\; \mathbf{e}_M \;\; \lambda\mathbf{e}_1\,]$, for some $\lambda \in \mathbb{C}$, where each vector $\mathbf{e}_m$ is an all-zero vector, except for a 1 in the $m$th position. The Sylvester operator $\nabla_{\mathbf{Z}_\eta,\mathbf{Z}_\xi}$ applied to a Toeplitz

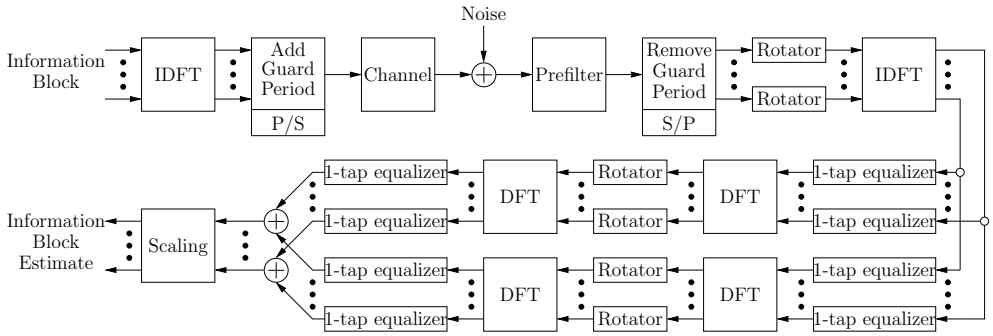


Fig. 1. DFT-based multicarrier system with minimum redundancy: ZF solution [7].

matrix $\mathbf{T}$ yields

$$\begin{aligned}\nabla_{\mathbf{Z}_\eta,\mathbf{Z}_\xi}(\mathbf{T}) &= \mathbf{Z}_\eta\mathbf{T}-\mathbf{T}\mathbf{Z}_\xi \\ &= \underbrace{\begin{bmatrix}1\\0\\\vdots\\0\end{bmatrix}}_{\hat{\mathbf{p}}_1}\underbrace{\begin{bmatrix}\eta t_{M-1}-t_{-1} & \cdots & \eta t_1 - t_{1-M} & \eta t_0\end{bmatrix}}_{\hat{\mathbf{q}}_1^T} \\ &\quad + \underbrace{\begin{bmatrix}-\xi t_0\\ t_{1-M}-\xi t_1\\ \vdots\\ t_{-1}-\xi t_{M-1}\end{bmatrix}}_{\hat{\mathbf{p}}_2}\underbrace{\begin{bmatrix}0 & 0 & \cdots & 1\end{bmatrix}}_{\hat{\mathbf{q}}_2^T} \\ &= \hat{\mathbf{p}}_1\hat{\mathbf{q}}_1^T+\hat{\mathbf{p}}_2\hat{\mathbf{q}}_2^T = [\,\hat{\mathbf{p}}_1\ \hat{\mathbf{p}}_2\,]\begin{bmatrix}\hat{\mathbf{q}}_1^T\\ \hat{\mathbf{q}}_2^T\end{bmatrix} = \hat{\mathbf{P}}\hat{\mathbf{Q}}^T. \quad (3)\end{aligned}$$

The former example shows how to compress a Toeplitz matrix. After this compression stage, several operations can be efficiently performed using well-known results from the displacement theory [6]:

$$\nabla_{\mathbf{Y},\mathbf{X}}(\mathbf{U}^{-1}) = -\mathbf{U}^{-1}\nabla_{\mathbf{X},\mathbf{Y}}(\mathbf{U})\mathbf{U}^{-1}, \quad (4)$$

$$\Delta_{\mathbf{X},\mathbf{Y}^{-1}}(\mathbf{U}) = -\nabla_{\mathbf{X},\mathbf{Y}}(\mathbf{U})\mathbf{Y}^{-1}, \quad (5)$$

$$\nabla_{\mathbf{X},\mathbf{Z}}(\mathbf{U}\mathbf{V}) = \nabla_{\mathbf{X},\mathbf{Y}}(\mathbf{U})\mathbf{V}+\mathbf{U}\nabla_{\mathbf{Y},\mathbf{Z}}(\mathbf{V}), \quad (6)$$

$$\nabla_{\mathbf{X},\mathbf{Y}}(\alpha\mathbf{U}+\beta\mathbf{V}) = \alpha\nabla_{\mathbf{X},\mathbf{Y}}(\mathbf{U})+\beta\nabla_{\mathbf{X},\mathbf{Y}}(\mathbf{V}), \quad (7)$$

for any scalars $\alpha$, $\beta$, and any 5-tuple $\{\mathbf{U},\mathbf{V},\mathbf{X},\mathbf{Y},\mathbf{Z}\}$ of complex-valued matrices with compatible dimensions and, when necessary, nonsingular.

To conclude our brief description of structured matrices, let us define the discrete Fourier and Hartley transforms. By defining four class of angles $\theta_{\rm I}(i,j)=2ij\pi/M$, $\theta_{\rm II}(i,j)=i(2j+1)\pi/M$, $\theta_{\rm III}(i,j)=(2i+1)j\pi/M$, and $\theta_{\rm IV}(i,j)=(2i+1)(2j+1)\pi/2M$, for $(i,j)\in\{0,1,\cdots,M-1\}^2$, the orthogonal DHT-$X$ matrix is [9]:

$$[\boldsymbol{\mathcal{H}}_X]_{ij}=\frac{\sin[\theta_X(i,j)]+\cos[\theta_X(i,j)]}{\sqrt{M}}, \quad (8)$$

whereas the unitary DFT-$X$ matrix is defined as [9]:

$$[\mathbf{W}_X]_{ij}=\frac{\sin[\theta_X(i,j)]-\jmath\cos[\theta_X(i,j)]}{\sqrt{M}}, \quad (9)$$

with $\jmath^2=-1$ and $X\in\{\rm I,II,III,IV\}$. Sometimes, we refer to $\mathbf{W}_{\rm I}$ as $\mathbf{W}_M$. These matrices enjoy superfast implementations requiring only $\mathcal{O}(M\log_2 M)$ numerical operations.

## IV. Low-Redundancy Transceivers

Inspired by the standard implementations of OFDM-based transceivers that decompose the circulant effective channel matrix by using DFT, IDFT, and diagonal matrices, we shall describe now the factorization of the inverse of the Toeplitz effective channel matrix $\mathbf{H}_0$ using diagonal matrices and superfast transforms, such as DFT and DHT.

### A. DFT-Based Transceivers

By applying the concepts of the displacement theory one can compress the effective channel matrix $\mathbf{H}_0$ similarly to the way performed in (3). After this compression stage, the compressed representation of $\mathbf{H}_0^{-1}$ can be obtained by using (4). The properties of the resulting compressed matrix can be exploited to conceive the following representation for the receiver matrix [7]:

$$\mathbf{G}_0=\frac{1}{2}\mathbf{F}_0^H\mathbf{W}_M^H\left(\sum_{r=1}^{R}\mathbf{D}_{\tilde{\mathbf{p}}_r}\mathbf{W}_M\mathbf{D}\mathbf{W}_M\mathbf{D}_{\tilde{\mathbf{q}}_r}\right)\mathbf{W}_M^H\mathbf{D}^H, \quad (10)$$

where $\mathbf{D}_{\mathbf{x}}=\operatorname{diag}\{\mathbf{x}\}$ for any vector $\mathbf{x}$, $\mathbf{D}=\operatorname{diag}\{e^{\jmath\frac{\pi}{M}m}\}_{m=0}^{M-1}$, and $\tilde{\mathbf{p}}_r$ and $\tilde{\mathbf{q}}_r$ are vectors that depend on $\mathbf{H}_0$. This dependency is expressed as a function of both $\mathbf{H}_0^{-1}$ and the Sylvester displacement of $\mathbf{H}_0$, namely $\nabla_{\mathbf{Z}_{-1},\mathbf{Z}_1}(\mathbf{H}_0)$.

The parameter $R$ defines the number of parallel branches used for equalization at the receiver end [7], [8], [9]. A ZF solution uses $R=2$ branches, whereas an MMSE solution uses $R=4$ branches. A single-carrier transceiver can be designed by setting $\mathbf{F}_0=\mathbf{I}$, whereas a multicarrier system can be designed by setting $\mathbf{F}_0=\mathbf{W}_M^H$ for both MMSE and ZF designs.

Fig. 1 depicts the resulting multicarrier transceiver structure for the ZF case. The prefilter can be used to shorten the channel and/or to modify some of its characteristics [2]. The $m$th phase shifter, or rotator, is defined as $e^{\pm\jmath\frac{\pi}{M}m}$. The single-tap equalizers contain the elements of the vectors $\tilde{\mathbf{q}}_r$ and $\tilde{\mathbf{p}}_r$.

### B. DHT-Based Transceivers

It is also possible to use real transform-based transceivers [9]. Among the advantages of using these transceivers, we can highlight the fact that multicarrier

systems may benefit greatly from using them along with real baseband modulations, such as PAM, since the transmission of inphase/quadrature (I/Q) independent data is not required, avoiding I/Q–imbalance problems. As a drawback, however, the proposed transceivers require the effective channel to be symmetric.

Similarly as described in Subsection IV-A, the receiver matrix can be decomposed as [9]:

$$\mathbf{G}_0 = \frac{M}{2}\mathbf{F}_0^T \boldsymbol{\mathcal{H}}_{\mathrm{III}} \left( \sum_{r=1}^{R} \mathbf{D}_{\tilde{\mathbf{p}}_r} \boldsymbol{\mathcal{H}}_{\mathrm{II}} \boldsymbol{\mathcal{H}}_{\mathrm{IV}} \mathbf{D}_{\tilde{\mathbf{q}}_r} \right) \boldsymbol{\mathcal{H}}_{\mathrm{IV}}, \qquad (11)$$

where, in this case, the single-carrier solution can be designed by setting $\mathbf{F}_0 = \mathbf{I}$, whereas the multicarrier solution can be designed by setting $\mathbf{F}_0 = \boldsymbol{\mathcal{H}}_{\mathrm{III}}$ for both MMSE ($R = 4$) and ZF designs ($R = 2$).

## V. Simulation Results

We transmit 200 data blocks carrying $M = 32$ symbols of a BPSK constellation. In fact, each data block stems from 16 data bits that, after channel coding (with constraint length 7, code rate $R_c = 1/2$, and octal generators $\mathbf{g_0} = [\mathbf{133}]$ and $\mathbf{g_1} = [\mathbf{165}]$) [7], yields 32 bits to be baseband modulated. We assume that both symbol and channel models use the sample frequency $f_s = 1.0$ MHz. We also consider that both synchronization and channel estimation are perfectly performed at the receiver end.

The throughput is computed by using a Monte-Carlo averaging process with $10,000$ simulations. For each new simulation, a new random Rayleigh channel with uniform power-delay profile is generated ($L = 30$). The computation of the throughput is based on the expression $\rho R_c M(1-\mathrm{BLER}) f_s/(M+K)$ bps, where $\rho$ is the number of bits required to represent one symbol in a given constellation, $R_c$ is the code rate, $K$ is the amount of redundancy ($L = 30$ for standard OFDM and $L/2 = 15$ for our proposals), $f_s = 1.0$ MHz is the sample frequency, and BLER is the block-error rate. We consider an error-free type of application, so that a block error is computed whenever at least one of the 16 data bits obtained after channel decoding is erroneously detected.

Let us focus on the DFT-based transceivers from now on. Fig. 2 depicts the throughput curves for the OFDM, the single-carrier with frequency-domain (SC-FD) equalization, the multicarrier minimum-redundancy block transceiver (MC-MRBT), and the single-carrier minimum-redundancy block transceiver (SC-MRBT), using both ZF and MMSE designs. By observing this figure it is possible to verify that the throughput performances of the proposed transceivers are much better than the traditional ones, except for SNRs lower than 12 dB in the ZF solutions. Note that such favorable result stems from the choices for $M$ and $L$ (delay constrained applications in very dispersive environments). These types of applications are suitable for the proposed transceivers. In the cases where $M \gg L$, the traditional OFDM and SC-FD solutions are more adequate.

In this simplified setup, it was observed an analogous behavior of the DHT-based transceivers. Hence, due to lack of space, we will omit the results related to these real transform-based transceivers.

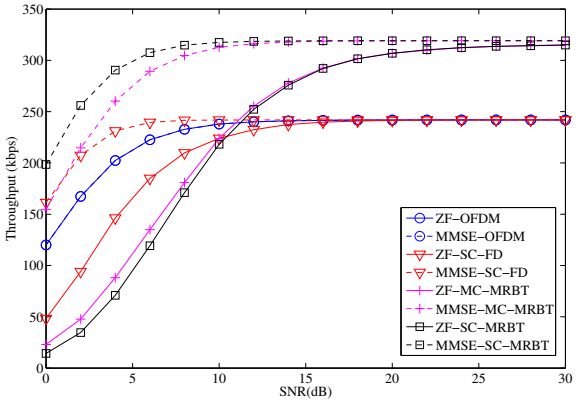


Fig. 2. Throughput as a function of SNR for random Rayleigh channels [7].

## VI. Concluding Remarks

This paper reviewed some recent advances of low-redundancy transceivers. The ZF and MMSE solutions were described for both multicarrier and single-carrier systems. The resulting transceivers employ only diagonal matrices, and DFT or DHT matrices. This is important to turn the new transceivers computationally efficient. All of these attractive features were achieved using the properties of structured matrices. Simulation results demonstrate that low-redundancy solutions allow higher throughput in a number of situations, revealing the potential usefulness of both DFT- and DHT-based transceivers.

## Acknowledgment

The authors thank CNPq for funding.

## References

[1] A. Scaglione, G. B. Giannakis, and S. Barbarossa, "Redundant filterbank precoders and equalizers part I: unification and optimal designs," *IEEE Trans. Signal Process.*, vol. 47, no. 7, pp. 1988–2006, Jul. 1999.

[2] Y.-P. Lin and S.-M. Phoong, "Minimum redundancy for ISI free FIR filterbank transceivers," *IEEE Trans. Signal Process.*, vol. 50, no. 4, pp. 842–853, Apr. 2002.

[3] C. B. Ribeiro, M. L. R. Campos, and P. S. R. Diniz, "FIR equalizers with minimum redundancy," *in Proc. IEEE Int. Conf. on Acoust. Speech and Signal Process.*, Orlando, Florida, May 2002, Vol. III, pp. 2673-2676.

[4] C. B. Ribeiro, M. L. R. Campos, and P. S. R. Diniz, "Time-varying FIR transmultiplexers with minimum redundancy," *IEEE Trans. Signal Process.*, vol. 57, no. 3, pp. 1113–1127, Mar. 2009.

[5] P. P. Vaidyanathan, S.-M. Phoong and Y.-P. Lin, *Signal Processing and Optimization for Transceiver Systems.* New York: Cambridge Univ. Press, 2010.

[6] V. Y. Pan, *Structured Matrices and Polynomials: Unified Superfast Algorithms*. New York, NY: Springer, 2001.

[7] W. A. Martins and P. S. R. Diniz, "Block-based transceivers with minimum redundancy," *IEEE Trans. Signal Process.*, vol. 58, no. 3, pp. 1321–1333, Mar. 2010.

[8] W. A. Martins and P. S. R. Diniz, "Suboptimal linear MMSE equalizers with minimum redundancy," *IEEE Signal Process. Letters*, vol. 17, no. 4, pp. 387–390, Apr. 2010.

[9] W. A. Martins and P. S. R. Diniz, "Minimum redundancy multicarrier and single-carrier systems based on Hartley transforms," *in Proc. 17th Eur. Signal Processing Conf.*, Glasgow, Scotland, Aug. 2009, pp. 661–665.

[10] W. A. Martins and P. S. R. Diniz, "Pilot-aided designs of memoryless block equalizers with minimum redundancy," *in Proc. IEEE Int. Symp. on Circuits and Systems*, Paris, France, May. 2009, pp. –.